International Journal of Advance Research in Science and Engineering
Volume No. 12, Issue No. 10, October 2023
www.ijarse.com
IJARSE
ISSN 2319 - 8354

Influence of Aluminium Doping on Energy Band-Gap and Photocatalytic Activity of TiO_2 Nanoparticles

Jyoti S.Bharambe[1], Prajkta Borgaonkar[2], V.B.Pujari[3]

1. Associate Professor, Physics Department,

ICLES' Motilal Jhunjhunwala College of Arts Science and Commerce, Vashi, Navi Mumbai,India

2. Assistant Professor, Physics Department

Vikas college of Arts, Science and Commerce, Vikhroli, Mumbai,India

3. Associate Professor, Physics Department,

Karmaveer Bhaurao Patil College, Vashi, Navi Mumbai, India

ABSTRACT

By employing the Sol-Gel method, pure and aluminium doped titanium dioxide (TiO_2) nanoparticles for various Al/Ti ratios were synthesized using titanium butoxide as a precursor. The samples were examined using micro-raman spectroscopy, scanning electron microscopy (SEM), energy dispersive X-ray spectroscopy (EDAX) and X-ray diffraction in order to obtain morphological and elemental analysis. With increasing dopant concentration, the crystallite size of undoped and Al-doped TiO_2 decreased from 9 nm to 6 nm. UV-Vis diffuse reflectance spectra were used to investigate optical characteristics, which demonstrated a shift in absorption spectra towards the visible range in Al-doped TiO_2, confirming the presence of dopant atoms. As the dopant concentration was increased, the band gap of TiO_2 nanoparticles was narrowed and lowered from 3.19 to 2.93 eV. A photodegradation efficiency of the prepared samples was determined by examining the methylene blue degradation. There was a significant increase in the efficiency of all Al-doped TiO_2 samples compared to pure TiO_2 nanoparticles. Among the doped samples, 3Al-TiO_2 nanoparticles exhibited the highest degradation efficiency.

KEYWORDS: *Al-TiO_2 nanoparticles, Sol-Gel, crystallite size, Band gap, Photodegradation, Methylene blue.*

1. Introduction

Photocatalysis is the most efficient method to clean wastewater, industrial effluents, environment and energy related developments. The photocatalysis is the activation of a chemical process by a photocatalyst irradiated by an UV-visible light source. A good photocatalyst needs to be affordable, nontoxic, photostable, chemically and biologically inert, capable to use visible and/or near UV light, and photoactive [1]. The principle of photocatalysis is based on activating a semiconductor by light with energy larger than its band gap, which results in the generation of electron-hole pairs [2]. It is well known that titanium dioxide (TiO_2) is one of the most effective photocatalysts due to its extraordinary properties, including its low cost, superior activity, high stability, nontoxicity, chemical

inertness and its optical and electrical properties [1][3][4]. The photocatalytic activity of depends on parameters such as morphology, band gap, surface area, and its crystalline structure [5]. TiO_2 photocatalyst mostly absorb ultraviolet light from the solar spectrum due to its wide energy band gap of around 3.2 eV [1][6]. The wide band gap of TiO_2 limits its practical application as a photocatalyst in the visible range, as it utilizes only 3-5% of solar radiation[7]. photocatalytic performance of TiO_2 is further restricted due to the high rate of electron-hole pair recombination [8]. A popular method of reducing the effective band gap directly is to dope TiO_2 with acceptor or donor impurities. Researchers have discovered that metal doped TiO_2 nanostructures can be an effective way to modify their electronic properties. Red-shifting the absorbtion edge towards visible light by decreasing the energy band gap is the main objective of doped TiO_2. By generating oxygen vacancies and electron trapping mechanisms, dopants can also enhance photocatalytic efficiency by preventing the rapid recombination of photogenerated electron-holes and enhancing their separation rate [9] [10][11].

There has been substantial research in recent years focused on modifying photocatalysts using semi-conductors doped with metal for improved photocatalytic action on various organic pollutants [12]. copper (Cu), Zinc (Zn), nickel (Ni), cobalt (Co), iron(Fe) manganese (Mn), barium (Ba) [13], Vanadium(V)[14] silver (Ag)[10], chromium (Cr), palladium (Pd), Aluminium (Al) [15] metal doped TiO_2 exhibited a red shift in the absorption edge, which boosted photocatalytic activity of TiO_2. D. Lee et al. synthesised Al-doped TiO_2 at various Al/Ti ratios and demonstrated that Al-doped TiO_2 had improved photocatalytic efficiency than pure TiO_2 [16].

This experiment aims to prepare undoped and Al doped Titanium dioxide nanoparticles (TiO_2) with different doping concentrations using conventional Sol-Gel technology, and study how doping concentration affects photodegradation efficiency of methylene blue dye solution..

2. Experimental

2.1 Synthesis pure and Al-doped TiO_2

The sol-gel process was used to synthesize aluminium-doped TiO_2 nanoparticles of various aluminium concentrations (Al/Ti =0.5%, 1% ,2%, 3%). During this process Titanium butoxide $[Ti(OC_4H_9)_4]$ (sigma,97%) was employed as a precursor while nitric acid (HNO_3) (sigma 70%) was used as a catalyst. To obtain solution A, 17 ml of Titanium butoxide was mixed with 40 ml of ethanol (C_2H_5OH) (Merck, 99%)and Aluminium nitrate (nonahydrate) ($Al(NO_3)_3$ $9H_2O$) (Merck, 99%) as a doping agent and stirred continuously at room temperature for 1 hour. For the preparation of solution B, 40 mL of ethanol was mixed with 5 mL of deionised water and 0.5 mL of nitric acid. The solution B, was then introduced drop by drop in the prepared solution A, while magnetic stirring for an hour. The resulting solution was stirred vigorously for another 1 hour at room temperature to improve homogeneity. Gelation was accomplished by keeping the solution at room temperature for 48 hours. Excess solvent was removed by heating at 100˚C for 3 hours and the resulting powders were then calcined at 500 ˚C for 2 hours after grinding them using a mortar and pestle.

The pure TiO_2 powder was synthesized by the same process without the addition of Aluminium nitrate (nonahydrate) in solution A.

2.2 Characterization

To study the phase and crystallinity of TiO_2 and Al-doped TiO_2, powder XRD (using Cu Kα radiations having wavelength 1.54056 Å in the range of 20˚ to 80˚. The average crystallite size was calculated from the by Scherrer's equation [3]:

$$D = \frac{0.9\lambda}{\beta\cos\theta}$$

Where D is the average crystallite size (nm), λ is the wavelength of the X-ray radiation, β is the full width at half maximum intensity and θ is the half diffraction angle. The anatase percentage of TiO_2 was computed using the Spurr equation[16]:

$$X_A = \frac{1}{1 + 1.26(I_R/I_A)}$$

A scanning electron microscope (SEM) (Vega3Tescan) provided with energy-dispersive spectroscope (EDAX) was employed to analyse the morphological characteristics of the surface and elemental composition of all of the samples. In order to confirm the phases and structure, a Raman spectrophotometer (Renishaw with a laser of a wavelength of 633 nm) has been utilized. With a Jasco V 760 NIR spectrophotometer, UV-VIS diffuse reflectance spectra within the range 200 nm-800 nm wavelength were obtained in order to estimate the band gap energy of all the samples.

To evaluate the photoactivity of the prepared TiO_2 nanomaterials, methylene blue was selected as a model organic compound. Under light irradiation, all the samples were tested for their photocatalytic activity by photodegrading Methylene Blue (MB) dye solution. 160 W Mercury vapour lamp was used as a radiation source for photodegradation. A mixture of 50 ml of aqueous MB (10mg/L) solution containing 5 mg of prepared photocatalyst was stirred into the glass beaker to conduct the photocatalytic degradation experiment. Adsorption-desorption equilibrium of the molecules in the solution was achieved by continuously stirring the suspension for 30 minutes. The light source was kept 10 cm away from the beaker. The solution was irradiated with the mercury source under constant stirring. An absorbance was obtained using a spectrophotometer by withdrawing two ml of the solution from the beaker in the cuvette. A plot of the normalized intensity obtained in the absorption band of Methylene Blue at wavelength 660 nm as a function of exposure time was used to analyse the photocatalytic activity of MB. The same procedure carried out without addition of catalyst is referred as blank reaction.

3. Result and Discussion

The XRD patterns of pure TiO_2 and Al-doped TiO_2 are shown in Fig. 1. The observed diffraction peaks at 2θ of 25.32°, 37.9°, 48.05°, 54.29°, 62.6°, 68.4° and 75.03° for pure TiO_2 are attributed to planes (101), (004), (200),

(105), (211), (116), (215) of anatase phase of TiO_2 (JCPDS file no. 21–1272) [17] and diffraction peaks at 2θ of 27.60° are attributed to planes (110) of rutile phase. In 0.5Al-TiO_2 additional small peaks at 36.20°and 41.62° attributed to the planes (101) and (111) of the rutile phase (JCPDS file no. 21–1276) [18] were also observed. Whereas 1Al-TiO_2, 2Al-TiO_2 and 3Al-TiO_2 showed diffraction peaks corresponding to anatase phase only. The crystallite size of the samples was calculated for the plane (101) by Sherrer's equation and was in the range of 9 nm to 6 nm which was slightly less than undoped TiO_2.The crystallite size decreased with the increase in the Al concentration in TiO_2 (Table 1.).

Interplaner spacing was determined by Bragg's law:

$$2d\sin\theta=n\lambda.$$

The d values calculated for the diffraction peaks are in good agreement with those given in JCPD data card. (JCPD no. 78-2485 and 78-2486)[19]. The lattice constant a, b and c in all the samples were determined by tetragonal unit cell formula:

$$\frac{1}{d^2}=\frac{h^2+k^2}{a^2}+\frac{l^2}{c^2}$$

and are tabulated in Table 1[20]. The lattice constant values confirmed the tetragonal structure of anatase phase of TiO_2, and matched with JCPDS file No.71-1167[21].

Table 1: d spacing Crystallite size, Anatase Percentage of pure, lattice constants , volume of unit cell and energy band gap of Al doped TiO_2 nanoparticles

Sample	d spacing (nm)	Crystallite size (nm)	Anatase (%)	Lattice constant a=b (nm)	Lattice constant c(nm)	Volume a*b*c $(nm)^3$	Energy band gap
TiO_2	0.3505	9	83	0.3782	0.9483	0.1357	3.19
0.5Al-TiO_2	0.3486	9.2	95	0.3753	0.9406	0.1325	3.18
1Al-TiO_2	0.3505	8.62	100	0.3773	0.9480	0.1350	3.16
2Al-TiO_2	0.3516	6.8	100	0.3783	0.9482	0.1357	3.06
3Al-TiO_2	0.3512	6	100	0.3783	0.9455	0.1353	2.93

International Journal of Advance Research in Science and Engineering
Volume No. 12, Issue No. 10, October 2023
www.ijarse.com
IJARSE
ISSN 2319 - 8354

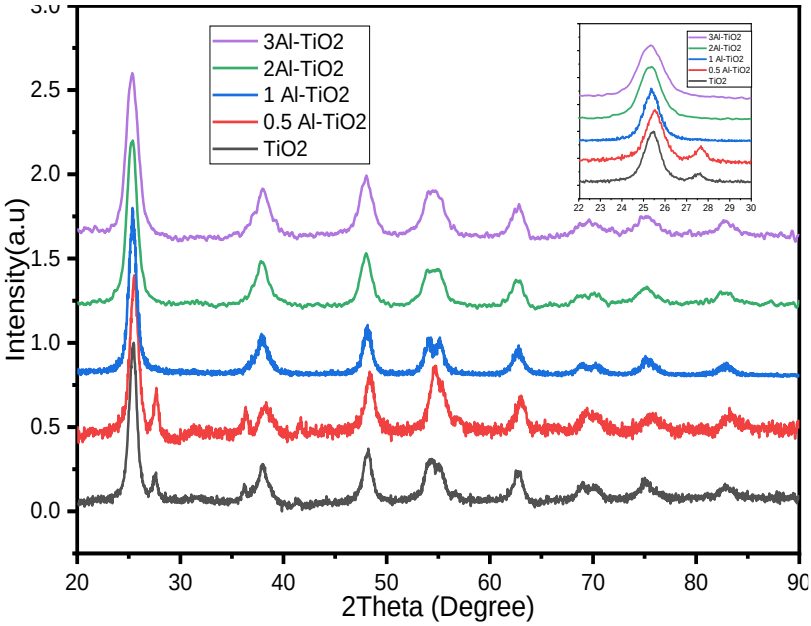

Fig. 1 X-ray diffraction pattern of Al-doped TiO_2 with different Al/Ti ratios

Raman spectra for pure and Al-doped TiO_2 recorded with 633nm laser, power 0.5 mW and for 100 sec acquisition time are shown in Fig. 2. Raman Spectra of pure TiO_2 shows peaks at 144, 195.8, 396.6, 516, 638.3 cm^{-1} corresponding to the Eg, E_g, B_{1g}, A_{1g}, and B_{2g} modes of anatase phase of TiO_2 respectively[22]. The peak positions of Al-doped TiO_2 samples at 147, 197, 400, 518, 640 cm^{-1} showed that the peaks are slightly shifted to higher position than pure TiO_2. The wider spectral lines implies that the crystallite size decreases with the increasing dopant concentration[23].

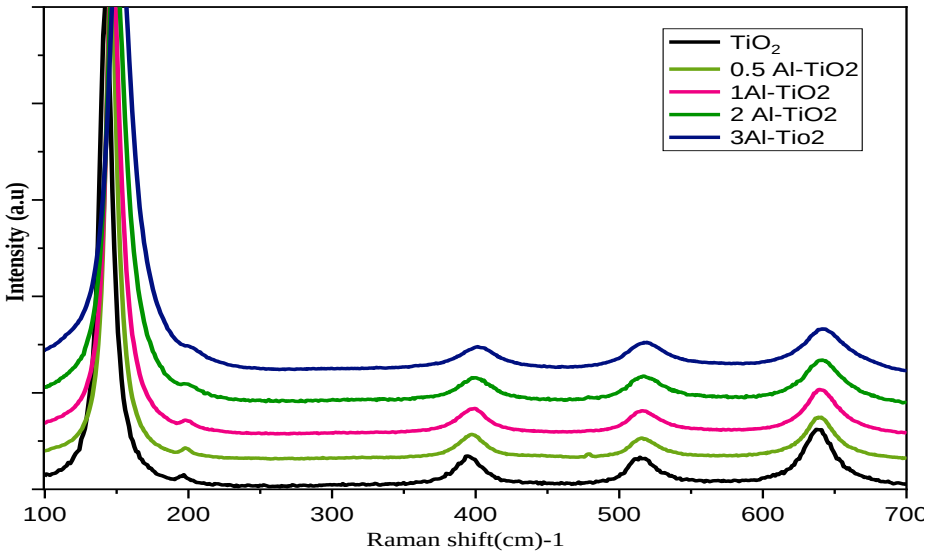

Fig. 2 Raman Spectra of pure and Al-doped TiO_2 nanoparticles with different Al concentrations

IJARSE
ISSN 2319 - 8354

The surface morphology of all the samples was obtained by scanning electron microscope (SEM) (Vega3Tescan) equipped with energy-dispersive spectroscopy. Fig. 3 shows SEM images of Al-doped TiO_2 for different dopant concentrations. Agglomerated particles have been observed to be arbitrarily dispersed across each of the prepared samples.

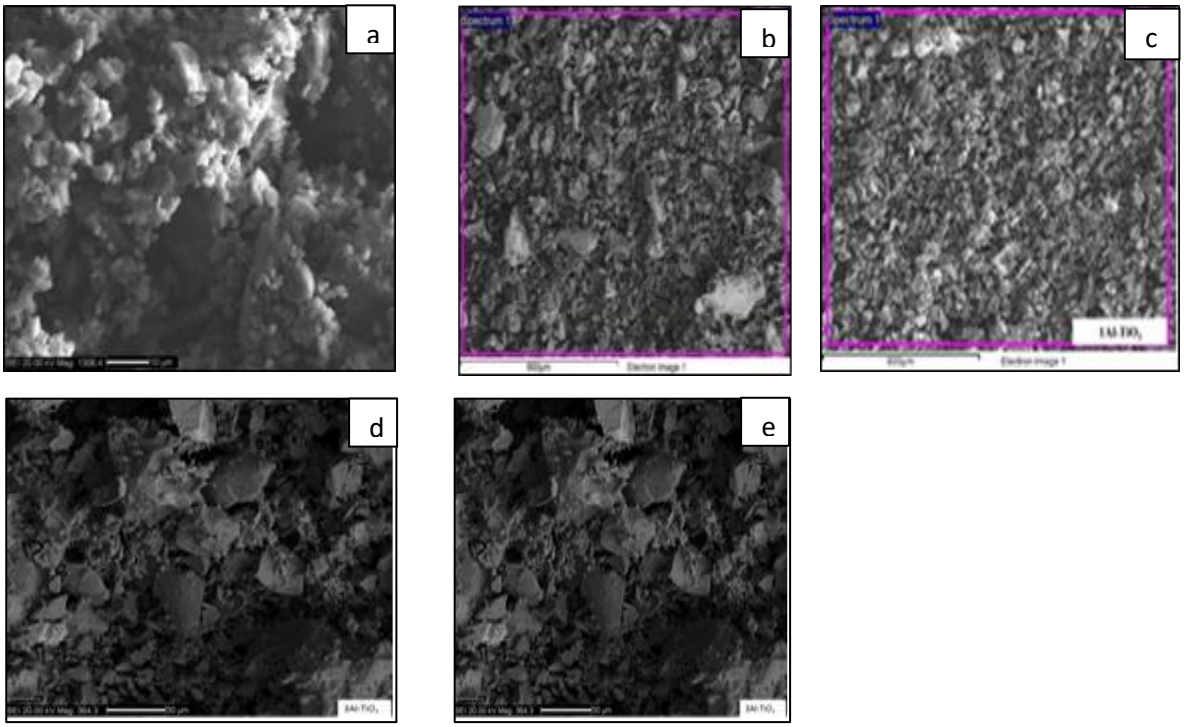

Fig3. SEM images of (a) TiO_2 (b) 0.5Al-TiO_2 (c) 1Al-TiO_2 (d) 2Al-TiO_2 e)3Al-TiO_2

The EDAX mapping of Al-doped TiO_2 for different dopant concentration are as shown in Figure 4. The EDAX spectra verified the elemental composition of Al, Ti, and O. The percentage of Al increases with increasing the dopant concentration resulting in the decrease in the the concentration of Ti into the TiO_2 lattice as shown in Table 2. Furthermore, the percentage of Al and Ti indicates the substitution of doping on the surface of the TiO_2 lattice. No other additional impurities are detected in the EDAX spectra.

Table 2. EDAX values of different doping concentrations of Al, Ti and O in TiO_2

Sample	TiO_2	0.5Al-TiO_2	1Al-TiO_2	2Al-TiO_2	3Al-TiO_2
	at%	at%	at%	at%	at%
Ti	28.12	24.57	29.76	22.74	22.79
O	71.88	75.21	69.64	75.98	75.26
Al	-	0.22	0.60	1.29	1.94
Total	100	100	100	100	100

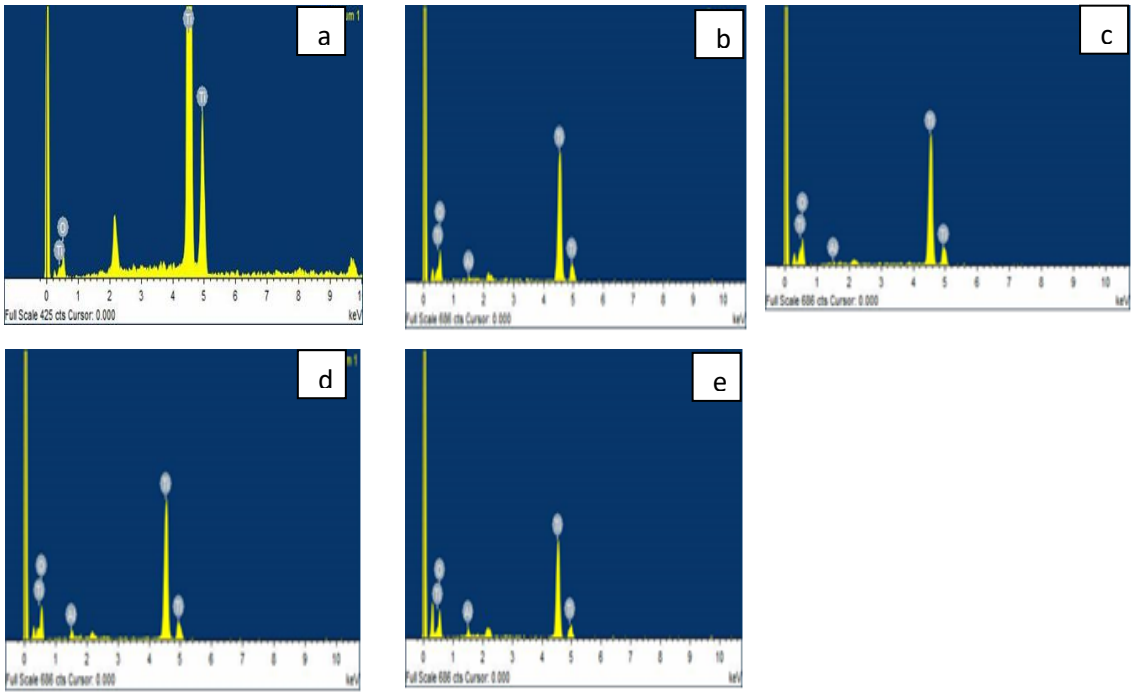

Fig. 4. EDAX spectra (a) TiO_2 (b) 0.5Al-TiO_2 (c) 1Al-TiO_2 (d) 2Al-TiO_2 (e)3Al-TiO_2 nanoparticles

The UV-vis absorption spectra of undoped TiO_2 and Al-doped TiO_2 nanoparticles with different doping concentrations are shown in Figure 5. The absorbance of the visible spectrum increases with an increase in the dopant ratio. The band gap values calculated Using Kubelka-Munk equation and extrapolating Tauc plot to the hν axis as shown in Figure 6. shows that the band gap energy decreases with increasing concentration of Al in TiO_2 from 3.19 eV of pure TiO_2 to 2.93eV (Table 1). The decrease in the band gap was due to the incorporation of Al^{+3}ions into TiO_2 crystal structure.

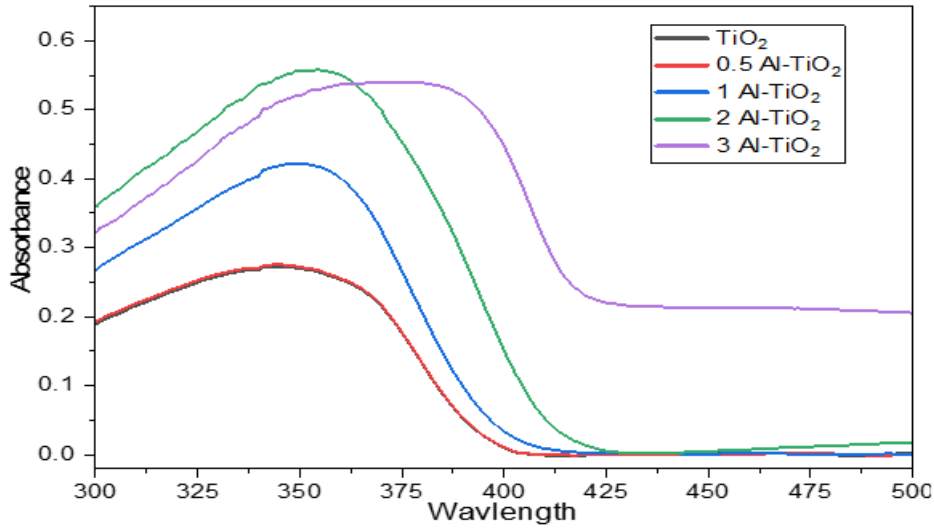

Fig. 5. Diffused reflectance spectroscopy of undoped TiO_2 and Al-doped TiO_2samples

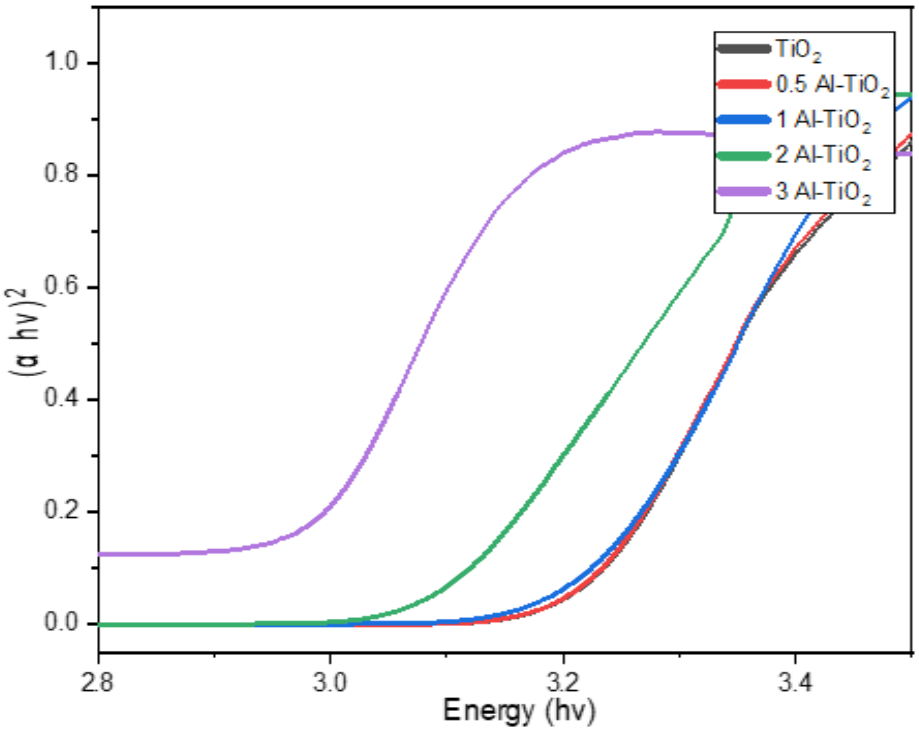

Fig. 6. Tauc plot of undoped TiO_2 and Al-doped TiO_2 samples

4. Photocatalytic Activity

In this experiment, Methylene Blue (MB) dye was used as the target compound to evaluate the photocatalytic activity of Al-doped TiO_2. Due to their carcinogenicity and toxicity dyes cause serious threats to the environment. The characteristic peak at 660 nm was obtained from the absorption spectrum of Methylene blue. Degradation of the MB dye was examined by measuring the relative peak intensity at 660 nm proir and after the introduction of TiO_2 under light irradiation. Fig. 7 shows photocatalytic activity of Al-doped TiO_2 samples for the degradation of the MB dye under the illumination of 160 watt mercury vapour lamp. The percentage photodegradation rate of MB dye using pure and Al-doped TiO_2 was calculated by the following equation:

$$\text{Photodegradation Rate (\%)} = \frac{Co-Ct}{Co} \times 100\%$$

where Co is the initial concentration of MB and Ct is the concentration of the MB when the photocatalytic reaction was completed in presence of visible light[24]. Pure TiO_2 and Al-doped TiO_2 samples were irradiated with a mercury lamp for the 100 % degradation of blue coloured methylene blue solution to produce colourless solution. The photocatalytic activity of all Al-doped TiO_2 samples was higher than pure TiO_2. Increased doping concentrations increased the photocatalytic activity and showed maximum photodegration rate for 3Al-TiO_2. A smaller crystallite size of Al doped TiO_2 samples increased the surface area which led to highest photocatalytic activity in 3Al-TiO_2 nanoparticles.

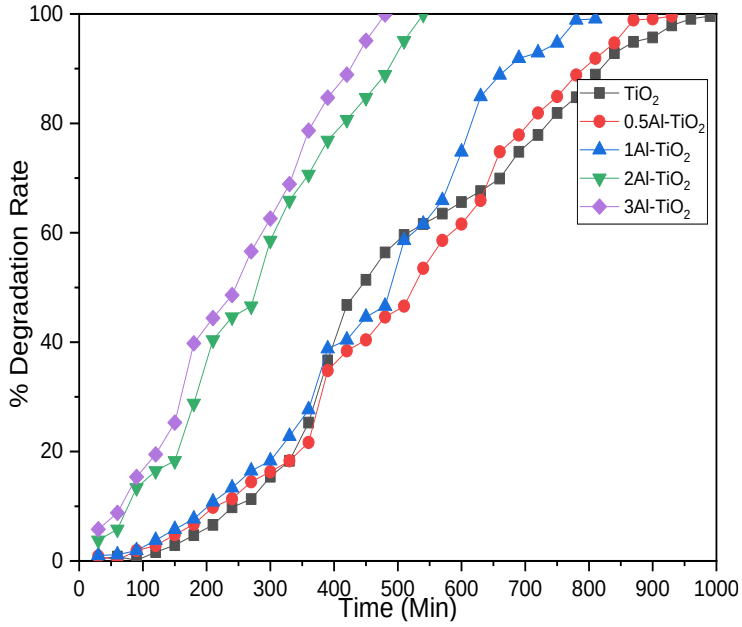

Fig. 7. Photodegradation of Methylene blue for pure and Al-doped TiO_2 samples illuminated by Mercury vapour lamp

5. Conclusion

This study reports the synthesis and characterization of pure and aluminium-doped TiO_2 nanoparticles using the sol-gel method at various dopant concentrations. All the samples were characterized by XRD, SEM, EDAX and RAMAN spectroscopy and confirmed the presence of Aluminium in anatase TiO_2. The crystallite size of pure TiO_2 was decreased from 9 nm to 6 nm with increase in the dopant concentration of aluminium dopant. EDAX spectra verified the elements Ti, O and Al in Aluminium doped TiO_2. Uv-vis DRS showed that absorption peak was shifted to visible region with higher concentration of Al in TiO_2. Energy band gap was determined by the tauc plot and which showed a decrease in the energy band gap from 3.19 eV to 2.93 eV with increasing Al concentration.The photocatalytic activity of pure and Al-doped samples was evaluated by the photodegradation of Methylene Blue in the presence of a Mercury lamp. The photodegradation rate was found to be improved for the higher concentration of Al dopant in TiO_2 due to the reduction in crystallite size and an increase in the surface area.

Overall, this study demonstrates that the sol-gel method can be effectively used to synthesize Al-doped TiO_2 nanoparticles with improved optical and photocatalytic properties, which could have potential applications in wastewater treatment.

REFERENCES

[1] S. C. A. Rakshit Ameta, “Binary Semiconductors,” *Photocatalysis, Principles and applications* (CRC Press, 2016, 17–34). doi: 10.1201/9781315372396-4.

[2] C. Belver, J. Bedia, A. Gómez-Avilés, M. Peñas-Garzón, and J. J. Rodriguez, "Semiconductor Photocatalysis for Water Purification," *Nanoscale materials in water purification* (Elsevier Inc., 2019, 581–651). doi:10.1016/B978-0-12-813926-4.00028-8.

[3] W. Zhou, Q. Liu, Z. Zhu, and J. Zhang, Preparation and properties of Vanadium-doped TiO2 photocatalysts, *J. Phys. D. Appl. Phys.*, *43(3)*, 2010, doi: 10.1088/0022-3727/43/3/035301.

[4] D. M. De Los Santos, J. Navas, A. Sánchez-Coronilla, R. Alcántara, C. Fernández-Lorenzo, and J. Martín-Calleja, Highly Al-doped TiO_2 nanoparticles produced by Ball Mill method: Structural and electronic characterization", *Mater. Res. Bull.*, *70*, 704–711, 2015. doi:10.1016/j.materresbull.2015.06.008.

[5] A. Castro-Beltrán *et al.*, Titanium butoxide molar ratio effect in the TiO_2 nanoparticles size and methylene blue degradation, *Optik (Stuttg).*, *157*, *January*, 890–894,2018, doi: 10.1016/j.ijleo.2017.11.185.

[6] R. Jaiswal, J. Bharambe, N. Patel, Alpa Dashora, D.C. Kothari, A. Miotello, Copper and Nitrogen co-doped TiO_2 photocatalyst with enhanced optical absorption and catalytic activity, *Applied Catalysis B: Environmental, 168-169* . 333-34,2015,doi: 10.1016/j.apcatb.2012.06.030.

[7] Z. J. Shi, M. G. Ma, and J. F. Zhu, Recent development of photocatalysts containing carbon species: A review, *Catalysts*, *9(1)*, 2019, doi: 10.3390/catal9010020.

[8] S. G. Kumar and L. G. Devi, Review on Modified TiO_2 Photocatalysis under UV / Visible Light : Selected results and related mechanisms on interfacial charge carrier transfer dynamics, *J. Phys. Chem. A*, *115(46)*, 2011, 13211–13241. https://doi.org/10.1021/jp204364a.

[9] R. Li, T. Li, and Q. Zhou, Impact of titanium dioxide (TiO_2) modification on its application to pollution treatment—a review, *Catalysts*, *10(7)*, 2020. doi: 3390/catal10070804.

[10] C. G. Wu, C. C. Chao, and F. T. Kuo, Enhancement of the photo catalytic performance of TiO_2 catalysts via transition metal modification,*Catal. Today*, *97 (2-3 SPEC. ISS)*., 103–112, 2004, doi: 10.1016/j.cattod.2004.04.055.

[11] M. L. Puga, J. Venturini, W. C. Guaglianoni, T. L. Ruwer, T. B. Wermuth, and P. Bergmann, Aluminium-doped TiO_2 nanotubes with enhanced light-harvesting properties, *Ceramics International*, *47(13)*, 18358-18366, 2021.

[12] Z. A. A. and A. A. Imran Ali, Mohd Suhail, Recent advances in syntheses , properties and applications of TiO_2 nanostructures, *RSC Adv.*, *2018(8)*, 30125-30147, doi: 10.1039/c8ra06517a.

[13] Y. N. Tan, C. L. Wong, and A. R. Mohamed, An Overview on the photocatalytic activity of nano-doped-TiO_2 in the degradation of organic pollutants, *ISRN Mater. Sci.*, *2011*, 1–18, 2011, doi: 10.5402/2011/261219.

[14] W. Avansi, R. Arenal, V. R. De Mendonça, C. Ribeiro, and E. Longo, Vanadium-doped TiO_2 anatase nanostructures: The role of v in solid solution formation and its effect on the optical properties, *CrystEngComm*, *16(23)*, 5021–5027, 2014, doi: 10.1039/c3ce42356e.

[15] A.V. Prasada Rao, A.M. Umabala and P. Suresh, Non-TiO_2 based photocatalysts for remediation of hazardous organic pollutants under green technology-present status: A Review, *Journal of Applicable*

Chemistry, 4 (4): 1145-1172,, 2016.

[16] D. Y. Lee, M. H. Lee, B. Y. Kim, and N. I. Cho, Crystal structure and photocatalytic activity of Al-doped TiO_2 nanofibers for methylene blue dye degradation, *J. Nanosci. Nanotechnol.*, *16(5*), 5341–5344, 2016, doi: 10.1166/jnn.2016.12273.

[17] A. El Mragui, Y. Logvina, O. Zegaoui, and J. C. G. Esteves, Synthesis of Fe- and Co-doped TiO_2 with improved photocatalytic activity under visible irradiation toward carbamazepine degradationphotocatalytic activity under visible irradiation toward carbamazepine degradation, *Green Chem.*, 18(4), 4–6, 2019.

[18] A. Sanchez-Martinez, C. Koop-Santa, O. Ceballos-Sanchez, Edgar R. López-Mena, M. A. González, V. Rangel-Cobián, E Orozco-Guareño and M. García-Guaderrama, Study of the preparation of TiO_2 powder by different synthesis methods, *Materials Research Express, 6(8)*, 2019.

[19] S.G. Pawar , M. A. Chougule , P. R. Godse , D. M. Jundale, S. A. Pawar, B. T. Raut, V. B. Patil, Effect of annealing on structure, morphology, electrical and optical properties of nanocrystalline TiO_2 thin films, *J. Nano- Electron. Phys.*, *3(1)*, 185–192, 2011.

[20] Y. Li, D. Xu, J. Il Oh, W. Shen, X. Li, and Y. Yu, Mechanistic Study of Codoped Titania with Nonmetal and Metal Ions : A Case of C + Mo Codoped TiO 2, *ACS Catal.*, *2(3*), 391–398, 2012, doi: doi.org/10.1021/cs2006668.

[21] Y. Wang, X. Su, and S. Lu, Shape-controlled synthesis of TiO_2 hollow structures and their application in lithium batteries, *J. Mater. Chem.*, *22(5)*, 1969–1976, 2012, doi: 10.1039/c1jm14637h.

[22] J. Yu, S. Nam, J. W. Lee, D. I. Kim, and J. Boo, Synthesis and characterization of vanadium doped TiO 2 for the visible light-driven photocatalytic activity, proceeding IEEE conc. on International Renewable and Sustainable Energy Conference (IRSEC), Marrakech, Morocco 2016, 14-17. DOI: 10.1109/IRSEC.2016.7984028, 14-17 Nov. 2016

[23] A. J. Maira, K. L. Yeung, C. Y. Lee, P. L. Yue, and C. K. Chan, Size effects in gas-phase photo-oxidation of trichloroethylene using nanometer-sized TiO2 catalysts, *J. Catal.*, *192(1)*, 185–196, 2000, doi: 10.1006/jcat.2000.2838.

[24] M. Zhang, J. Wu, D. Lu, and J. Yang, Enhanced visible light photocatalytic activity for TiO_2 nanotube array films by codoping with tungsten and nitrogen," *Int. J. Photoenergy*, *2013*, 2013. doi:10.1155/2013/471674.